CrossMark click for updates

Nano-patterning of the electron gas at the $LaAlO_3/SrTiO_3$ interface using low-energy ion beam irradiation

Pier Paolo Aurino,[1,a)] Alexey Kalabukhov,[1,2] Nikolina Tuzla,[3] Eva Olsson,[3] Tord Claeson,[1] and Dag Winkler[1]

[1]*Department of Microtechnology and Nanoscience - MC2, Chalmers University of Technology, SE-412 96 Gothenburg, Sweden*
[2]*Skobeltsyn Institute of Nuclear Physics, Department of Physics, Moscow State University, 119899 Moscow, Russia*
[3]*Department of Applied Physics, Chalmers University of Technology, SE-412 96 Gothenburg, Sweden*

(Received 25 March 2013; accepted 8 May 2013; published online 24 May 2013)

The quasi-two dimensional electron gas formed at the interface between $LaAlO_3$ (LAO) and $SrTiO_3$ (STO) shows fascinating properties, such as two-dimensional superconductivity, giant electric field effect, and the possible co-existence of ferromagnetic and superconducting phases. In this work, we demonstrate that the conducting LAO/STO interface can be made insulating after short irradiation by a beam of low energy Ar+ ions. The irradiation process does neither result in physical removal of the LAO film nor produces oxygen vacancies in the STO layer. Using electron beam lithography and low ion beam energy irradiation, we fabricated conducting nano-structures in the LAO/STO interface with dimensions down to 50 nm. Such a reliable and robust method of nano-patterning may be a prerequisite for future electronic applications of the LAO/STO interface.
© *2013 AIP Publishing LLC*. [http://dx.doi.org/10.1063/1.4807785]

High electrical conductivity and mobility at the interface between the two insulating Perovskite oxides $LaAlO_3$ and $SrTiO_3$ (LAO/STO) have been reported.[1] A quasi-two dimensional electron gas (q2DEG) appears at the LAO/STO interface only when 4 or more unit cells (uc) of LAO film are epitaxially deposited on TiO_2-terminated STO substrates.[2,3] The origin of the electrical conductivity at the LAO/STO interface is still not fully understood. Polar discontinuity at the interface,[4] presence of oxygen vacancies in the STO substrate,[5–7] or La-Sr intermixing[8] have been considered as possible models to explain electrical properties of the LAO/STO interface. However, the exact relationship between any of the proposed models and microstructure of the interface has not yet made clear.

The interface shows two-dimensional superconductivity below 200 mK,[9] giant electric field effect,[2] and possible co-existence of ferromagnetic and superconducting phases.[10,11] These properties make the LAO/STO interface an exciting model system for studying fundamental physics of strongly correlated electronic systems. Therefore, a reliable and robust technique for patterning of the q2DEG at the LAO/STO interface is required. A straightforward way is to physically remove the LAO film by chemical or dry etching, or using a lift-off process. Chemical etching of the LAO film is rather complicated as it is difficult to find durable materials that will resist aggressive acids required for the etching of the LAO film.[12] Ion beam etching is hampered by formation of oxygen vacancies in the STO substrate that results in electron doping of the interface shunting useful properties of the q2DEG.[13,14] Lift-off processes do not require etching of the LAO film, but very high temperature (800 °C) and oxygen atmosphere used during the deposition of the LAO film prohibit standard lift-off techniques with polymer resist layers. As an alternative solution, several hard lift-off masks have been suggested. An amorphous LAO mask was deposited at room temperature on the top of 2 uc of epitaxial LAO layer. A second deposition of a thicker epitaxial LAO film (>4 uc) was performed and conducting paths were formed only where the amorphous film was removed by the lift-off process.[15] Structures down to 200 nm could be produced using this method, but it requires two depositions of LAO film at high temperature. In another approach, a hard AlO_x film was used as a lift-off layer.[16] The possible risk associated with this method is that the surface of the substrate has to be exposed to chemicals before the deposition of the LAO film and this may affect the electronic properties of the interface electron gas or limit practical resolution.

Conducting tip atomic force microscope (AFM) was used to "write" conducting paths in the LAO/STO interface without physical etching of the LAO film.[17] The method utilizes an electric field effect in a 3 uc non-conducting LAO/STO interface. Conducting paths could be written with very high precision down to a few nanometers by applying a local voltage using the AFM tip. However, the technique is difficult to scale up for fabrication of large area devices and showed limited durability.[17]

In this report, we show that it is possible to use argon ion beam irradiation to pattern the q2DEG at the LAO/STO interface by careful tuning of the beam energy and dose. The main finding of our work is that at low ion beam energy the electrical conductivity is eliminated faster than oxygen vacancies are created in the STO substrate. Therefore, by adjusting the irradiation dose, one can make the interface insulating and avoid unwanted electron doping due to the oxygen vacancies. Ion beam irradiation in combination with optical and electron beam lithography was used to fabricate conducting nanostructures in the q2DEG with dimensions

[a)]Author to whom correspondence should be addressed. Electronic mail: aurino@chalmers.se. Tel.: +46(0)317723286. Fax: +46(0)317723471.

 © 2013 AIP Publishing LLC

down to 50 nm. All fabricated structures demonstrated excellent electrical transport properties down to low temperature and long-time stability. We also present structural investigations of irradiated samples using scanning transmission electron microscopy (STEM) and discuss possible mechanisms of the metal-insulator transition induced by ion beam irradiation.

Thin LAO films (from 4 to 10 uc) were grown on TiO_2-terminated STO substrates by pulsed laser deposition (PLD) from a single crystal LAO target.[18] The laser energy density was set at 1.5 J/cm^2 and the laser spot area on the target was 2 mm^2. The substrate was heated to 800 °C, and the oxygen deposition pressure was set to 10^{-4} mbar. The epitaxial growth was monitored using *in situ* reflection high-energy electron diffraction (RHEED). The RHEED showed clear intensity oscillations for all the samples confirming layer-by-layer growth. After the deposition, the samples were annealed for 1 h at 600 °C and 500 mbar of pure oxygen. The AFM imaging of the samples after deposition confirmed smoothness of surfaces and presence of clear 1 uc high terraces.

Ti/Au contacts (20 nm Ti and 120 nm Au) were fabricated by lift-off technique and dc magnetron sputtering. This method provides low-ohmic contact resistance to the LAO/STO interface. The ion beam irradiation was performed in an Oxford Ionfab 300 Plus system using an inductive coupled plasma Ar+ ion beam source and a 3 cm beam aperture. Samples were mounted on a stainless steel holder at an angle of 0° or 30° relative to the ion beam direction. The sample resistance was monitored *in situ* during the etching process in a two-point configuration using a Keithley 2400 source meter with 10 μA probe current. AFM was performed using Bruker ICON AFM in non-contact mode.

Electrical transport measurements were made in a "Quantum Design Physical Property Measurement System" (PPMS) in the temperature range of 2–300 K and in magnetic fields up to 14 T.

Cross section TEM samples were prepared for TEM and high angle annular dark field (HAADF) scanning TEM (STEM) analysis of the atomic structure of the interfaces. A FEI Tecnai TEM/STEM operated at 200 kV and a FEI Titan 80-300 TEM/STEM with a probe C_s corrector operated at 300 kV were used for the studies.

We first performed measurements of the electrical resistivity of the q2DEG in the LAO/STO *in situ* with Ar+ ion irradiation as a function of beam energy and dose. Fig. 1 shows the resistance of three different 10 uc thick LAO on STO samples as a function of Ar+ ion irradiation dose for three different beam voltages of 150, 250, and 350 V. A constant beam current density of 0.14 mA/cm^2 was used corresponding to a dose rate of 9×10^{14} Ar+ cm^{-2} s^{-1}. The incident angle between the ion beam and sample surface was set to 30°. For all samples, the resistance rapidly increases in the beginning of irradiation. For the 150 V beam voltage, the resistance becomes immeasurably high after about 1–2 min (corresponding ion dose about 1×10^{17} Ar+ cm^{-2}). For higher beam energies, the resistance starts to increase without reaching the measurement limit and decreases again to similar or lower values than before irradiation. This suggests that the ion irradiation creates oxygen vacancies in the STO

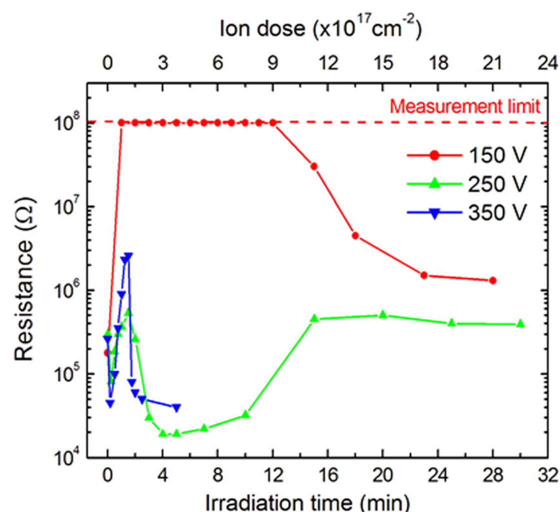

FIG. 1. Electrical resistance as a function of irradiation time for non-patterned 10 unit cell thick $LaAlO_3/SrTiO_3$ samples at three different beam voltages of 150, 250, and 350 V.

substrate. It is well known that oxygen vacancies donate electrons in the conducting band of the STO and result in n-doping.[19] The electron doping due to oxygen vacancies decreases the electrical resistance after longer irradiation times. It takes much longer time for the electrical resistivity to appear again for lowest beam energy and this leaves a possibility to utilize this time interval for the patterning of the q2DEG at the LAO/STO interface. Monte-Carlo simulations have confirmed that Ar+ ions with lowest energy are effectively stopped in the thin LAO film and do not create oxygen vacancies in the STO substrate, in well agreement with experimental findings.[20]

We also investigated the time dependence of resistance during low energy (150 V) ion beam irradiation of samples with different LAO film thicknesses. It showed that time required to obtain the insulating state increases with the film thickness: conductivity disappeared after 1 min of irradiation for 5 uc thick film, after 2 min for 10 uc thick film, and after 10 min for 15 uc thick film (for 150 V beam voltage).

Patterning of the LAO/STO interface was performed using photo and e-beam lithography and low-energy Ar+ ion beam irradiation. Ti/Au electrical contacts were fabricated in a first step by magnetron sputtering, and then samples were patterned and finally irradiated for 5 min at 150 eV by a beam of Ar+ ions. We also checked that there is no electrical conductivity between disconnected structures on the surface at all sizes proving again that irradiation indeed does not result in oxygen vacancy doping in the unprotected STO substrate. We also did not observe any degradation of the electrical properties of fabricated structures during several months.

Two types of structures were fabricated in the 10 uc thick LAO/STO samples: bridges of various width and Hall bars. Bridges have fixed aspect ratio (L:w = 5:1, where L is the length and w is the width) and widths in the range between 0.05 and 16 μm. All bridges were oriented at 0° relative to the substrate crystallographic axis. Hall bars had line width of 30 μm. AFM topography images of the surfaces of two patterned samples, ion irradiated at 30° and 0° angle

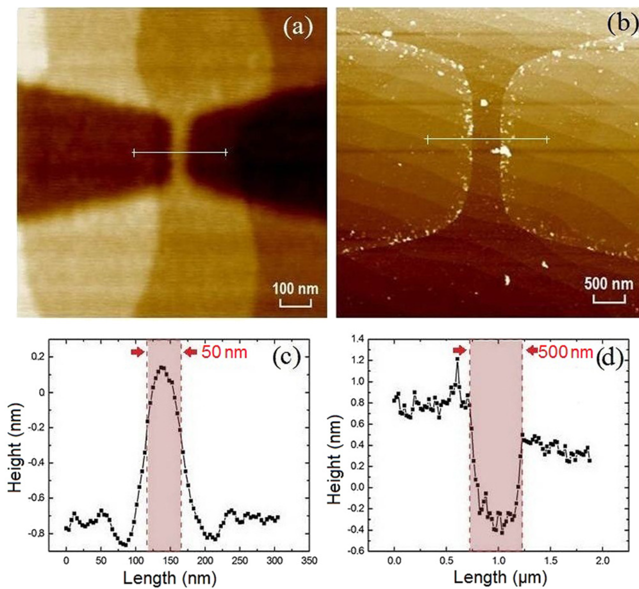

FIG. 2. AFM topography images of samples irradiated with (a) 30° and (b) 0° angles (relative to sample normal). (c) and (d) show line scans, and expected dimensions. Note that sputtering removes atoms (and decreases height) by 30° irradiation while 0° incidence gives minimal sputtering and increased height by amorphous "swelling". The marked region denotes the area protected by the resist.

incident beam, are shown in Figs. 2(a) and 2(b), correspondingly. The sample shown in Fig. 2(a) was produced by electron-beam lithography while photolithography was used to fabricate the sample shown in Fig. 2(b). The irradiated areas are clearly identified by the presence of residuals from the resist at the edge of the pattern, see Fig. 2(b). We noticed that the samples are more contaminated after the e-beam lithography process. In this case, we have cleaned the surface by scanning the AFM tip in contact mode across the surface, which resulted in a very clean surface of the sample, see Fig. 2(a).[21]

Line-scan traces of the AFM images in Figs. 2(a) and 2(b) are shown in Figs. 2(c) and 2(d), correspondingly. The step height difference between the irradiated (5 min) and protected areas in the LAO film is around 1–1.5 nm for 30° incident angle. This is much less than the nominal thickness of the film (∼4 nm). The corresponding etching rate of the LAO film can thus be estimated to about 0.2–0.3 nm/min. In the case of 0° incident beam angle, the irradiated areas increased in height by 0.5 nm compared to protected ones. This is most probably due to the fact that the film was not physically etched but instead made amorphous at this angle of incidence. The increase of the etching rate at higher angles is expected from an angular dependence of the sputtering yield.[22] We emphasize that the electrical conductivity was eliminated in both samples independent on the incident beam angle.

Electrical measurements of Hall bars showed high reproducibility of sheet resistance (50 kΩ/□) and charge carrier concentration ($1.5 \times 10^{13}\ \mathrm{cm}^{-2}$) within each Hall bar and between different Hall bars on the same sample. It was also found that the electron mobility measured in the patterned Hall bar structures is higher (up to $7000\ \mathrm{cm}^2\ \mathrm{V}^{-1}\ \mathrm{s}^{-1}$) as compared with the mobility measured in the 4-point Van der Pauw configuration performed on the same sample prior to patterning ($3000\ \mathrm{cm}^2\ \mathrm{V}^{-1}\ \mathrm{s}^{-1}$).

All fabricated nano-structures showed metallic behavior down to at least 2 K, see Fig. 3(a). The dependence of the sheet resistance as a function of bridge width is shown in Fig. 3(b). There is a notable increase of the sheet resistance with decreasing dimension of the structures. The sheet resistance is almost constant in bridges with width above 1 μm, but increases by a factor of 5 in 50 nm bridges.

The size of the bridges was estimated from both AFM topography and Kelvin probe images.[20] Simulations made with "Stopping and Range of Ions in Matter" (SRIM) simulation software[23] showed that the possible under-etching effect of the beam at corresponding energy is less than 4 nm and this would not explain the increase in sheet resistance in 50 nm wide bridges. Moreover, the size of the under-etched width can also be estimated to be maximum 25 nm, since bridges with width down to 50 nm show electrical conductivity. Assuming that the under-etching is constant in all fabricated structures, this does not explain the increase of the resistivity in 1 μm wide bridges. This suggests that the observed increase in the resistivity in small structures may be related to an inhomogeneous distribution of the electrical conductivity at the LAO/STO interface. At the same time, the spread of the sheet resistance is not as high as may be expected for an inhomogeneous conducting electron gas patterned below the percolation limit. Therefore, the exact nature of this effect requires further investigations.

In order to understand the mechanism of the metal-insulator transition after ion beam irradiation, we made STEM imaging that allows investigation of the structure of the film down to the interface (Fig. 4). Cross section TEM

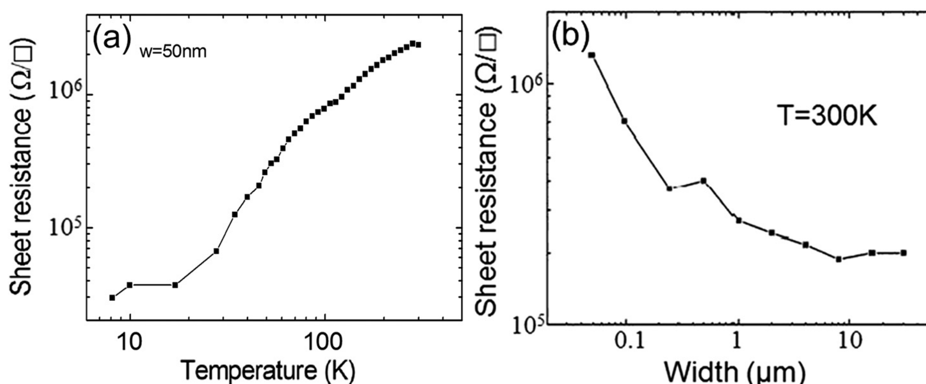

FIG. 3. (a) Temperature dependence of electrical resistance of 50 nm wide bridge patterned in the 10 uc LAO/STO interface. (b) Electrical transport properties of conducting structures in the LAO/STO interface fabricated by Ar+ ion beam irradiation. Sheet resistance of bridges as a function of their width.

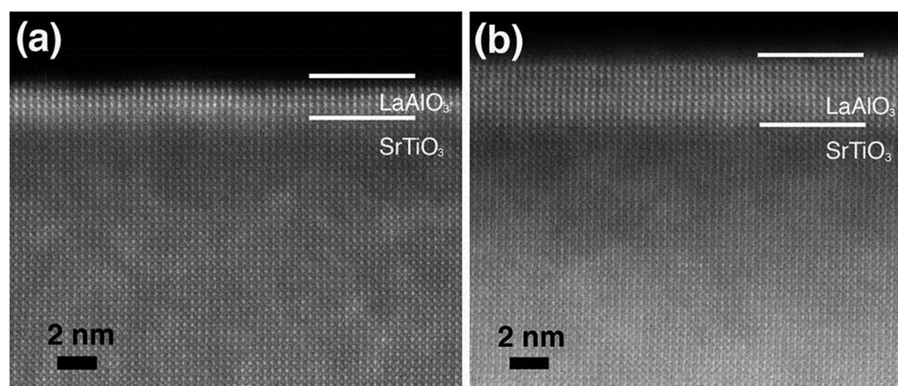

FIG. 4. HAADF STEM images of the 10 uc LAO/STO interface: (a) after 5 min irradiation by Ar+ ion beam at U = 150 V at 30° ion incidence and (b) without irradiation.

samples were prepared for TEM and HAADF STEM analysis of the atomic structure of the interfaces. To ensure that the TEM and STEM images were representative for the film, about 300 nm long fractions of the film along the interface were investigated in each of four specimens from four different locations. The analysis showed that the irradiated 10 uc thick LAO film has a crystalline structure with a thickness of 5–6 uc (Fig. 4(a)). This indicates that the crystalline film thickness is not reduced below the 4 unit cell critical threshold for electrical conductivity after the ion beam irradiation. This conclusion is also supported by the AFM imaging that showed very smooth surface of irradiated areas. There is no obvious difference in crystalline quality of the sample before (Fig. 4(b)) and after (Fig. 4(a)) the ion beam irradiation. We also checked if the interface electrical conductivity can be restored by a post annealing of the irradiated sample.[20] However, the sample remained insulating after the post annealing. STEM imaging, post-annealing experiment, and film thickness dependence of the time required to reach the insulating state, suggest that ion beam irradiation should not affect the polar structure of the interface. From STEM, it is also evident that film thickness is not reduced below the critical value. Other possible mechanisms can be related to local defects produced in the STO substrate during ion beam irradiation or Ar ion implantation in the LAO film.

In conclusion, we have demonstrated that low-energy Ar+ ion beam irradiation can be used for scalable and durable nano-patterning of the q2DEG at the LAO/STO interface avoiding the formation of oxygen vacancies in the STO substrate. The method is advantageous when compared to other techniques as it does not require hard masks or aggressive chemicals and the dimension of fabricated structures is limited by the resolution of the mask in the protective resist layer; conducting structures with dimensions down to 50 nm were fabricated using electron beam lithography masks and ion irradiation. This method opens possibilities for realization of quantum devices and electronic circuits based on complex oxide interfaces.

We greatly appreciate M. Hagberg from Nanofabrication Laboratory at Chalmers University of Technology for the help with ion beam etching and P. Hyldgaard from the Department of Microtechnology and Nanoscience, Chalmers University of Technology for valuable discussions. The work was supported by the Swedish Research Council, The Knut and Alice Wallenberg foundation, and Swedish Institute Visby program. The support from the Swedish Infrastructure for Micro- and Nanofabrication Myfab is appreciated.

[1]A. Ohtomo and H. Y. Hwang, Nature **427**, 423–426 (2004).
[2]S. Thiel, G. Hammerl, A. Schmehl, C. W. Schneider, and J. Mannhart, Science **313**, 1942–1945 (2006).
[3]N. Reyren, S. Thiel, A. D. Caviglia, L. Fitting-Kourkoutis, G. Hammer, C. Richter, C. W. Schneider, T. Kopp, A.-S. Räuetschi, D. Jaccard, M. Gabay, D. A. Muller, J.-M. Triscone, and J. Mannhart, Science **317**, 1196–1199 (2007).
[4]N. Nakagawa, H. Y. Hwang, and D. A. Muller, Nature Mater. **5**, 204–209 (2006).
[5]W. Siemons, G. Koster, H. Yamamoto, W. A. Harrison, G. Lucovsky, T. H. Geballe, D. H. A. Blank, and M. R. Beasley, Phys. Rev. Lett. **98**, 196802 (2007).
[6]A. Kalabukhov, R. Gunnarsson, J. Börjesson, E. Olsson, T. Claeson, and D. Winkler, Phys. Rev. B **75**, 121404(R) (2007).
[7]Y. Chen, N. Pryds, J. E. Kleibeuker, G. Koster, J. Sun, E. Stamate, B. Shen, G. Rijnders, and S. Linderoth, Nano Lett. **11**, 3774–3778 (2011).
[8]P. R. Willmot, S. A. Pauli, R. Herger, C. M. Shleputz, D. Martoccia, B. D. Patterson, B. Delley, R. Clarke, D. Kumah, C. Cionca, and Y. Yacoby, Phys. Rev. Lett. **99**, 155502 (2007).
[9]S. Gariglio, N. Reyren, A. D. Caviglia, and J.-M. Triscone, J. Phys.: Condens. Matter **21**, 164213 (2009).
[10]L. Li, C. Richter, J. Mannhart, and R. C. Ashoori, Nat. Phys. **7**, 762–766 (2011).
[11]J. A. Bert, B. Kalisky, C. Bell, M. Kim, Y. Hikita, H. Y. Hwang, and K. A. Moler, Nat. Phys. **7**, 767–771 (2011).
[12]We used concentrated phosphoric acid (H_3PO_4) at temperature around 130 °C. This provided etching rate of the LAO film of about 1 nm/min.
[13]D. Kan, T. Terashima, R. Kanda, A. Masuno, K. Tanaka, S. Chu, H. Kan, A. Ishizumi, Y. Kanemitsu, Y. Shimakawa, and M. Takano, Nature Mater. **4**, 816–819 (2005).
[14]H. Gross, N. Bansal, Y. S. Kim, and S. Oh, J. Appl. Phys. **110**, 073704 (2011).
[15]C. W. Schneider, S. Thiel, G. Hammerl, C. Richter, and J. Mannhart, Appl. Phys. Lett. **89**, 122101 (2006).
[16]N. Banerjee, M. Huijben, G. Koster, and G. Rijnders, Appl. Phys. Lett. **100**, 041601 (2012).
[17]C. Cen, S. Thiel, G. Hammerl, C. W. Schneider, K. E. Andersen, C. S. Hellberg, J. Mannhart, and J. Levy, Nature Mater. **7**, 298–302 (2008).
[18]M. Kawasaki, K. Takahashi, T. Maeda, R. Tsuchiya, M. Shinohara, O. Ishiyama, T. Yonezawa, M. Yoshimoto, and H. Koinuma, Science **266**, 1540–1542 (1994).
[19]H. P. R. Frederikse, W. H. Thurber, and W. R. Hosler, Phys. Rev. **134**, A442–445 (1964).
[20]See supplementary material at http://dx.doi.org/10.1063/1.4807785 for SRIM results, Kelvin Probe AFM measurements, and RHEED analysis.
[21]N. Lindvall, A. Kalabukhov, and A. Yurgens, J. Appl. Phys. **111**, 064904 (2012).
[22]J. J. Cuomo, S. M. Rossnagel, and H. R. Kaufman, *Handbook of Ion Beam Processing Technology-Principles, Deposition, Film Modification and Synthesis* (William Andrew Publishing/Noyes, 1989), p. 82.
[23]J. Ziegler, J. Biersack, and U. Littmark, *The Stopping of Ions in Matter* (Pergamon, New York, 1985).